Supplementary Information

Efficient Sr-90 removal from highly alkaline solution by a ultrastable crystalline zirconium phosphonate

Jiarong Zhang,‡[a,b] Long Chen,‡[c] Xing Dai,[c] Lixi Chen,[c] Fuwan Zhai,[c] Weifeng Yu,[d] Shikai Guo,[d] Lijiang Yang,[d] Lanhua Chen,[c] Yugang Zhang,[c] Linwei He,[c] Changlun Chen*[a,b], Zhifang Chai[c] and Shuao Wang*[c]

[a]*Institute of Plasma Physics, HFIPS, Chinese Academy of Sciences, P.O. Box 1126, Hefei 230031, P. R. China. E-mail: clchen@ipp.ac.cn.*
[b]*University of Science and Technology of China, Hefei 230026, P. R. China.*
[c]*State Key Laboratory of Radiation Medicine and Protection, School for Radiological and Interdisciplinary Sciences (RAD-X) and Collaborative Innovation Center of Radiation Medicine of Jiangsu Higher Education Institutions, Soochow University, Suzhou 215123, China. E-mail: shuaowang@suda.edu.cn.*
[d]*The 404 Company Limited China National Nuclear Corporation, Jiayuguan 735100, China.*
‡ *These authors contributed equally to this work.*
* *shuaowang@suda.edu.cn; clchen@ipp.ac.cn.*

Table of Contents

Methods and Experiments

Table S1. Crystallographic data for complexes.

Table S2. Bond distances of SZ-7.

Table S3. Bond Valence Sum (BVS) calculations O atoms.

Table S4. The equilibrium time and adsorption capacity for different materials in Sr^{2+} adsorption.

Table S5. Chemical composition of the simulated SRS tank waste sample used for test.

Table S6. ^{90}Sr sorption results of SZ-7 by liquid scintillation counting in simulated SRS waste.

Figure S1. Powder X-ray diffraction patterns of SZ-7.

Figure S2. The asymmetric unit of SZ-7.

Figure S3. The thermogravimetric analysis data of SZ-7.

Figure S4. Powder X-ray diffraction patterns of SZ-7 after treatment with aqueous solutions with different pH values.

Figure S5. Powder X-ray diffraction patterns of SZ-7 samples after β radiation.

Figure S6. Powder X-ray diffraction patterns of SZ-7 samples after γ radiation.

Figure S7. Pseudo-second-order model for Sr^{2+} uptake by SZ-7.

Figure S8. Comparison of the Sr^{2+} removal capacity (q) by SZ-7 with other Sr-adsorbents at different pH values.

Figure S9. Thermodynamic calculations on the equilibrium speciation of Sr^{2+} at alkaline condition.

Figure S10. Ion-exchange column made with SZ-7 composite used in the column experiment.

Figure S11. EDS data and SEM images of SZ-7.

Figure S12. EDS data and SEM images of Sr-loaded SZ-7.

Figure S13. Powder X-ray diffraction patterns of experimental Sr-loaded SZ-7 samples.

Methods and Experiments

Materials: All chemical reagents and solvents were received from commercial suppliers. ***Caution!*** Sr-90 is a high-energy β emitter. All Sr-90 experiments were performed in an authorized laboratory designed for radiological studies and provided standard protections for radioactive materials.

X-ray Crystallography Studies: Single crystal X-ray diffraction data of SZ-7 was collected on a Bruker D8-Venture diffractometer with a Turbo X-ray Source (Mo–Kα radiation, λ = 0.71073 Å) and a CMOS detector under 298 K. The data of SZ-7 was collected using the program APEX3 and then processed using SAINT routine in APEX3. SHELXTL was used to solve and refine the structure of SZ-7 by direct methods.

Characterizations: Powder X-ray diffraction (PXRD) patterns were collected from 5° to 50° with a step of 0.02° on a Bruker D8 Advance diffractometer with Cu Kα radiation (λ=1.54056 Å) and a Lynxeye one-dimensional detector. Thermogravimetric analyses were performed on a NETZSCH STA449F3 instrument in the range of 30-900 °C with a heating rate of 10 K/min under a nitrogen flow for the dried SZ-7. Scanning electron microscopy images and energy-dispersive spectroscopy data (SEM/EDS) of SZ-7 were collected on a FEI Quanta 200FEG Scanning Electron Microscope with the energy of the electron beam being 30 keV. SZ-7 samples were directly placed on the carbon conductive tape, and then

coated with Au. The concentration of nonradioactive Sr^{2+} was determined by inductively coupled plasma-atomic emission spectrometry (ICP-AES, Thermo Fisher Scientific iCAP 7000) or inductively coupled plasma-mass spectrometry (ICP-MS, Thermo Finnigan high resolution magnetic sector Element 2) depending on the specific concentration. Meanwhile, the concentration of radioactive $^{90}Sr^{2+}$ in solution was measured using liquid scintillation counting system (LCS). X-ray photoelectron spectroscopy (XPS) spectra were collected with a KratosAxis UltraDLD spectrometer using a monochromatic Al Kα source (1486.6eV) and the samples for XPS analysis were prepared in the batch experiments.

Synthesis of SZ-7: SZ-7 was synthesized by a solvothermal reaction. The mixture of 0.15 mmol (48.3 mg) of $ZrOCl_2 \cdot 8H_2O$ and 0.25 mmol (94.5 mg) of p-Xylenebis(diethyl phosphonate) dissolving in 2 mL of N,N-dimethylacetamide (DMA), 0.5 mL of H_2O, 0.15 mL HNO_3 solution (68%) and 0.05 mL HF solution (40wt%) was placed in a Teflon-lined stainless steel reactor and heated at 210 °C for 3 d, and then cooled to 30 °C at a rate of 22.5 °C h^{-1}. The precipitated solid was separated and washed with ethanol, and then dried at 60℃. Finally, colourless crystals were obtained as a pure phase.

Stability Measurements: Hydrolytic stability of SZ-7 was studied by stirring the samples in HNO_3 or NaOH solutions with different pH from 0 to 14 for 12 h. The solids were re-collected and treated for PXRD patterns

analysis. β irradiation resistance experiment was implemented using electron beams (1.2 MeV) provided by an electron accelerator. SZ-7 was irradiated for two different doses of 100 and 200 kGy at a dose rate of 20 kGy/h. γ irradiation experiment was carried out using a ^{60}Co irradiation source (2.22×10^{15} Bq) in the similar dose. PXRD patterns of irradiated SZ-7 samples were then collected to evaluate the irradiation stability.

Sr^{2+} Sorption Experiments: All the experiments were carried out at room temperature using the batch method. The solid/liquid ratio in nonradioactive batch experiments was 1 g/L. In a typical ion-exchange experiment of SZ-7, 10 mg SZ-7 was added into 10 mL aqueous solution containing certain Sr^{2+}. The mixture was kept stirring for 12 h. The concentration of Sr^{2+} in solution was determined by inductively coupled plasma mass spectrometry (ICP-MS) and/or inductively coupled plasma-atomic emission spectrometry (ICP-AES). The solids were separated by centrifugation or filtration. The distribution coefficient K_d is given by the equation:

$$K_d = (V[(C_0 - C_e)/C_e])/m$$

where V is the volume (mL) of the testing solution, C_0 and C_e are the initial and equilibrium concentration of Sr^{2+} (mg L^{-1}), and m is the amount of the SZ-7 samples (g) used in the experiment.

Kinetics Experiments: In the kinetics study, 30 mg of SZ-7 material was added into a 30 mL solution containing 10 ppm Sr^{2+}. The mixture was

then stirred by a magnetic bar for a desired contact time and then the concentration of Sr^{2+} as a function of time was obtained to determine the exchange kinetics line.

Adsorption Isotherm: The Sr^{2+} removal from solutions of various concentrations of 0-400 mg/L were investigated at the solid/liquid of 1 g/L stirring for 12 h at room temperature. The data were used for the determination of Sr^{2+} adsorption isotherm curve.

Competitive experiment: Competitive ion-exchange experiments of SZ-7 were also performed with the batch method at the solid/liquid of 1 g/L with the contact time of 12 h at room temperature. Specifically, 10 mg SZ-7 samples were stirred with 10 mL solutions containing 5 mg/L Sr^{2+} with the Na^{+}/K^{+} : Sr^{2+} molar ratio of 10:1, 100:1, 1000:1, 5000:1, and 10000:1 and 20000:1, respectively.

Column experiment: Column experiment was performed at auto solid phase extraction system (Sepaths UP4) with 70 mg SZ-7 samples packed into 3 mL column. The removal ratio was evaluated using aqueous solutions of 5 mg/L Sr^{2+} at a flow rate of 1 mL/min.

HLW adsorption experiment: The **radioactive** ^{90}Sr removal performance from simulated SRS tank waste with a total β activity of 455 cpm were further studied by adding SZ-7 samples to 3 mL ^{90}Sr solutions with different solid-liquid ratios of 1:1, 5:1, 10:1, and 15:1. The mixtures

were placed on a shaker for 12 h, followed by analysis using the LSC technique.

Table S1. Crystallographic data for complexes.

Sample	SZ-7
CCDC No.	2082185
Formula	$[(CH_3)_2NH_2]_2[ZrC_6H_4(CH_2PO_3)_2F_2]$
*M*r[g mol^{-1}]	461.32
Crystal system	triclinic
Space group	$P\ \bar{1}$
a (Å)	5.3254(10)
b (Å)	8.7035(16)
c (Å)	11.343(2)
α	92.747(10)
β	102.575(10)
γ	107.729(10)
V (Å^3)	485.05(16)
Z	1
D_c (g cm^{-3})	1.579
F (000)	224
T(K)	296(2)
R1,[a] ($I>2\sigma(I)$)	0.0995, 0.2750
R1,[a] (all data)	0.1314, 0.2953

[a] $R_1 = \sum(F_o - F_c)/\sum F_o$; $wR_2 = [\sum w(F_o^2 - F_c^2)^2/\sum w(F_o^2)^2]^{1/2}$

Table S2. Bond distances of SZ-7

Sample	Bond type	Distance(Å)	Bond type	Distance(Å)
SZ-7	Zr1-F1	1.987(6)	N1···O1 (Hydrogen bond)	2.928
	Zr1-O1	2.056(8)		
	Zr1-O2	2.075(8)		

Table S3. Bond Valence Sum (BVS) calculations O atoms.[1]

Atom	BVS value	Bond type
O1	1.91	Zr-O-P
O2	2.04	Zr-O-P
O3	1.32	P=O

Table S4. The equilibrium time and adsorption capacity for different materials in Sr^{2+} adsorption.

Compound	Experimental conditions	Equilibrium time	q (mg/g)	Ref
FJISM-SnS	T=290 K;1 g/L; pH∼7	60 min	65.19	2
KMS-1	1 g/L	>2 h	77	3
KMS-2	T=298 K; 1 g/L; pH=6.9	10-15 h	86.89	4
KTS-3	T=298 K; 1 g/L Neutral pH	>5 min	102	5
ETS-4	T=298 K; 4 g/L pH=5.9	24 h	201.5	6
MST	T=293 K; 10 g/L pH=5	>24 h	121.3	7
Zeolite A	T=298 K; 1 g/L pH=6	90-120 min (20-60 ^{o}C)	69.78	8
Go-Hap	T=298 K; 0.5 g/L pH=7.0±0.1;	2 h	702.18	9
SZ-4	T=298 K; 1 g/L; pH=4	20 min	129.8	10
FJSM-InMOF	T=298 K;1 g/L	2040 min	43.83	11
Nd-BTC	T=298 K; 0.05 g pH=8	30 min	58	12
MOF-808-C_2O_4	T=293 K;1 g/L; pH=4	120	206.34	13
SZ-7	**T=298 K; 1 g/L; Neutral pH**	**5 min**	**129**	**This work**

Table S5. Chemical composition of the simulated SRS tank waste sample used for test.[14]

Compound	Concentration (mol/L)*
$Sr(NO_3)_2$	1.8×10^{-4}
KNO_3	7.42×10^{-3}
NaOH	1
$NaNO_3$	3.73
$NaNO_2$	0.49
NaCl	1.33×10^{-2}
Na_2SO_4	4×10^{-2}
Na_2HPO_4	6.87×10^{-2}
Radioactive Compound	Activity (CPM)
$^{90}Sr^{2+}$	455

*The components with concentrations below 0.001 M were excluded.

Table S6 ^{90}Sr sorption results of SZ-7 by liquid scintillation counting in simulated SRS waste.

Phase ratio(mg/mL)	^{90}Sr activity
1	25
5	34
10	23
15	22

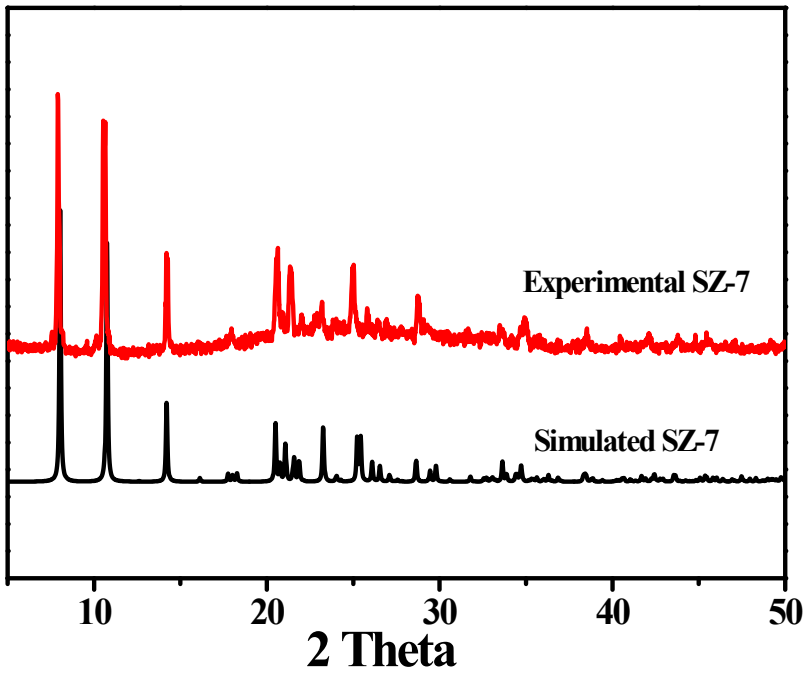

Figure S1. Powder X-ray diffraction patterns of SZ-7.

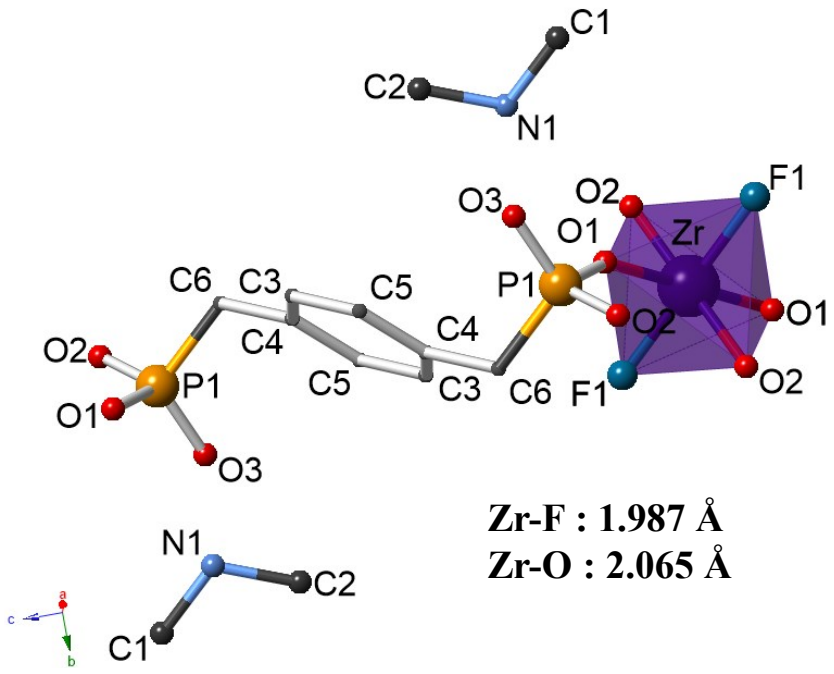

Figure S2. The asymmetric unit of SZ-7.

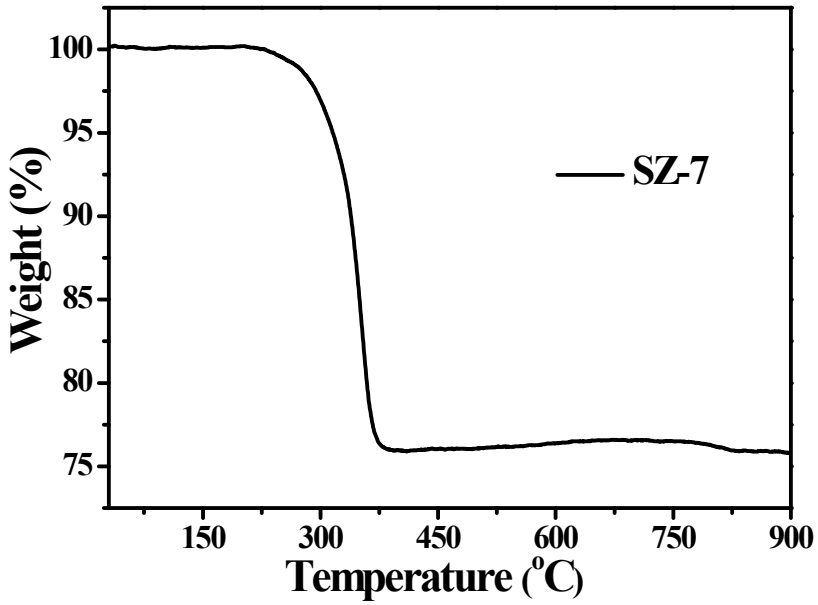

Figure S3. The thermogravimetric analysis data of SZ-7.

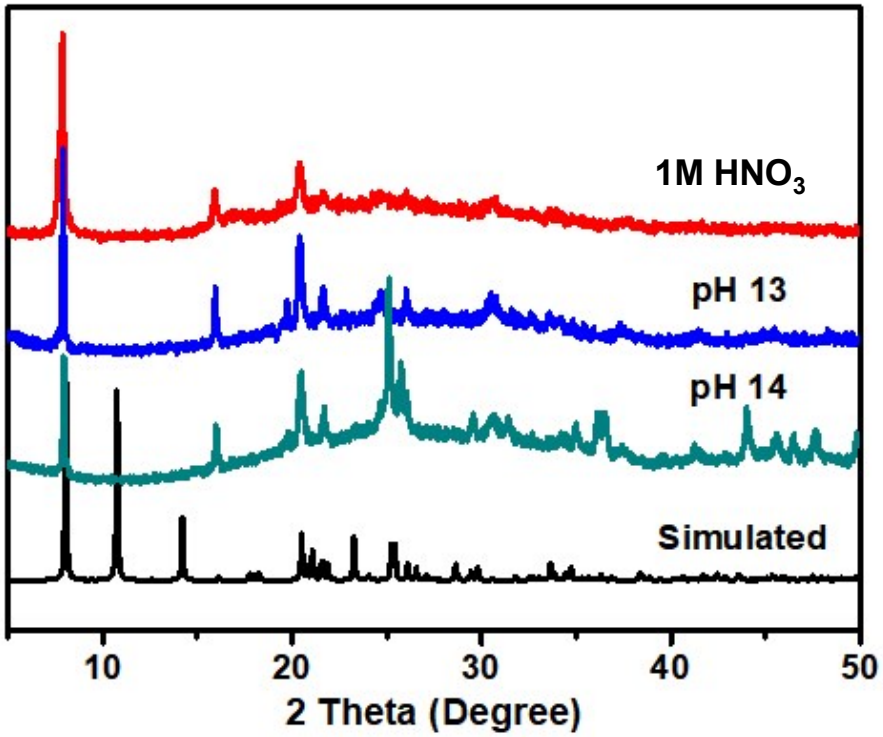

Figure S4. Powder X-ray diffraction patterns of SZ-7 after treatment with aqueous solutions with different pH values.

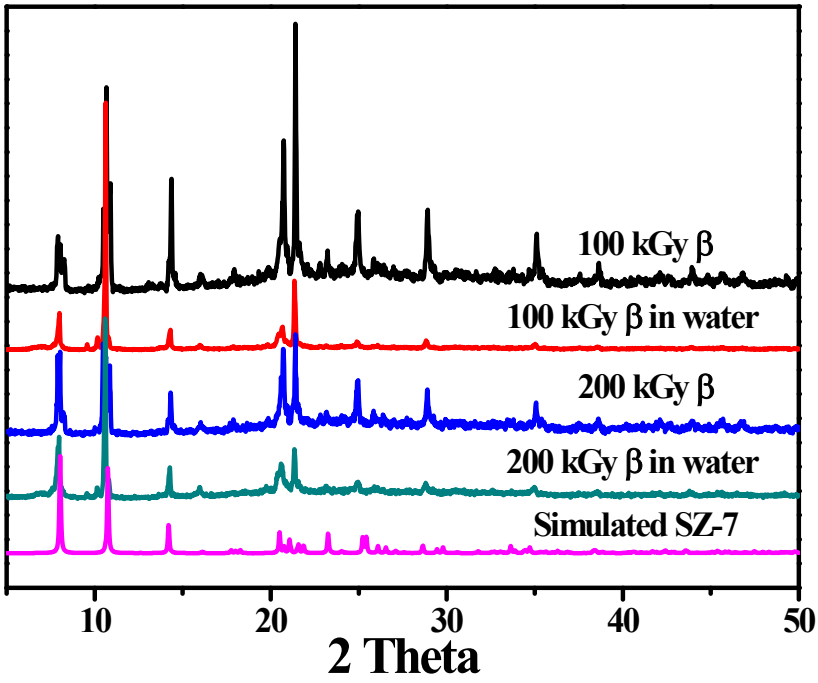

Figure S5. Powder X-ray diffraction patterns of SZ-7 samples after β radiation.

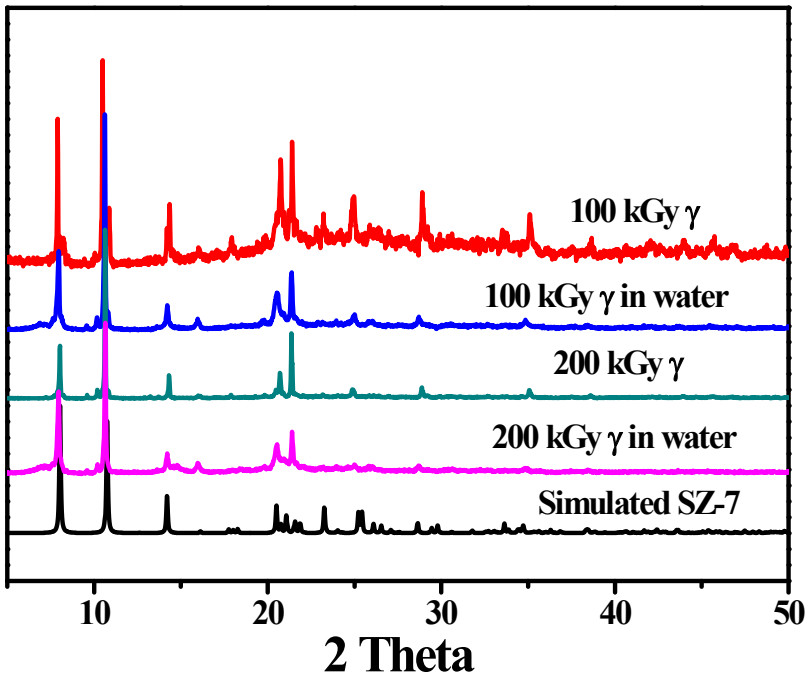

Figure S6. Powder X-ray diffraction patterns of SZ-7 samples after γ radiation.

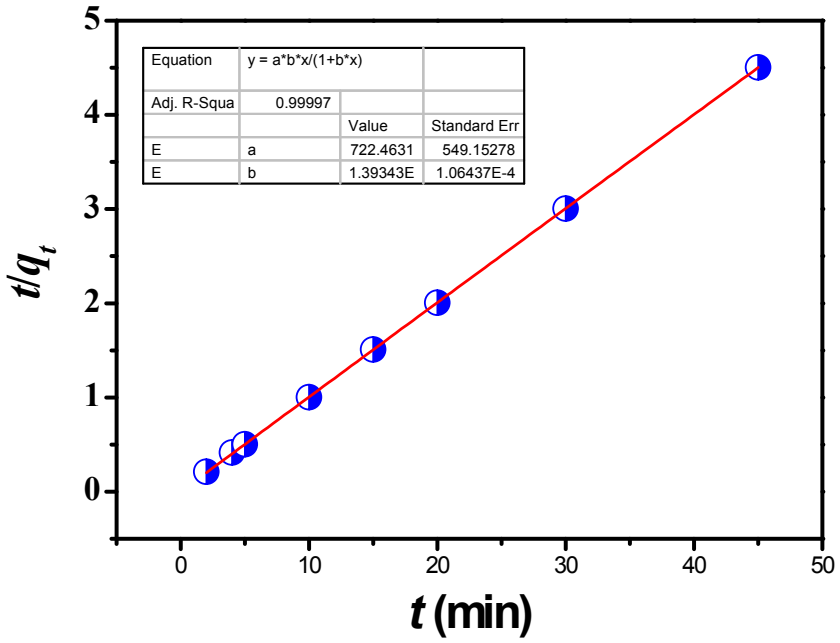

Figure S7. Pseudo-second-order model for Sr^{2+} uptake by SZ-7.

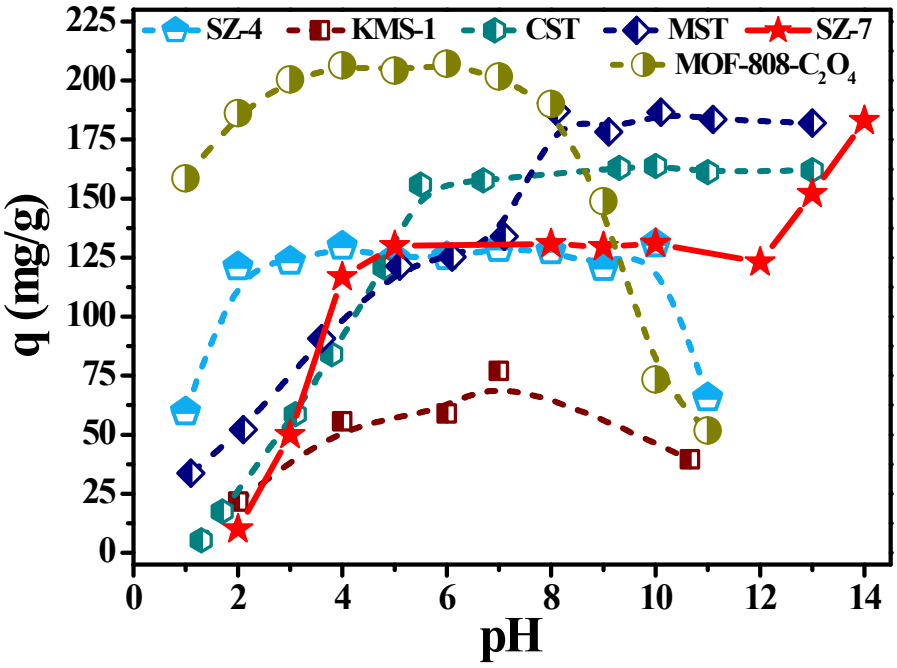

Figure S8. Comparison of the Sr^{2+} removal capacity (q) by SZ-7 with other Sr-adsorbents at different pH values.

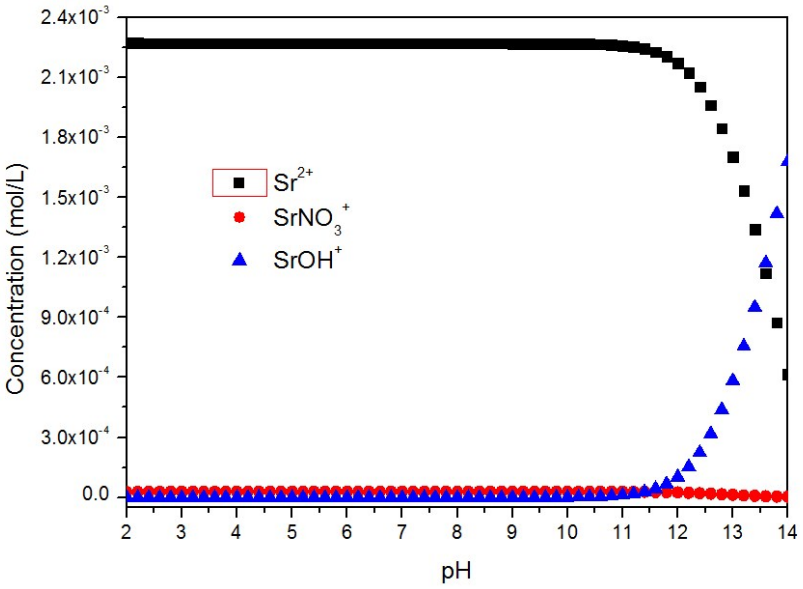

Figure S9. Thermodynamic calculations on the equilibrium speciation of Sr^{2+} at alkaline condition.

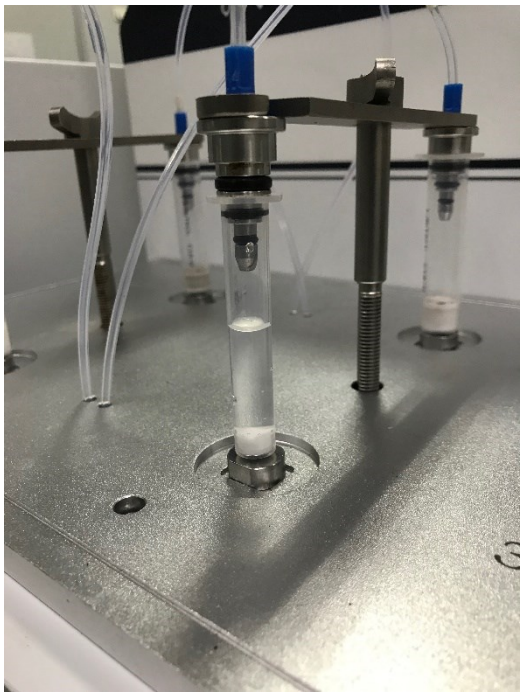

Figure S10. Ion-exchange column made with SZ-7 composite used in the column experiment.

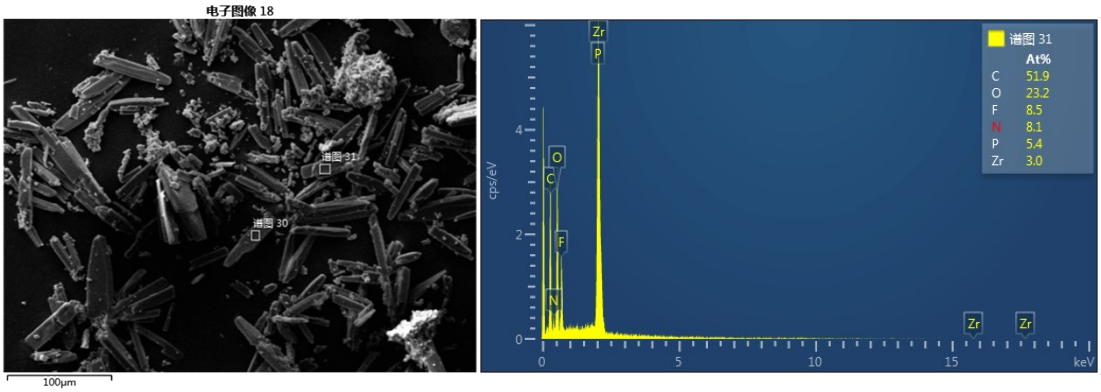

Figure S11. EDS data and SEM images of SZ-7.

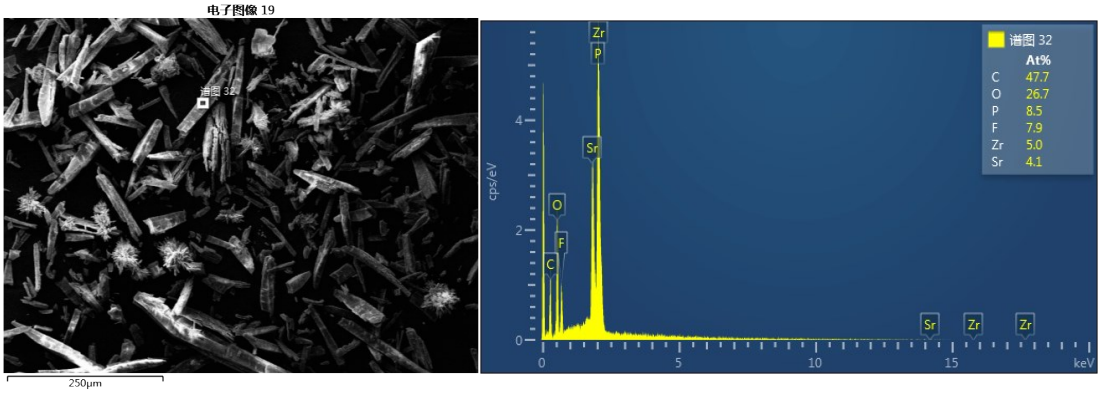

Figure S12. EDS data and SEM images of Sr-loaded SZ-7.

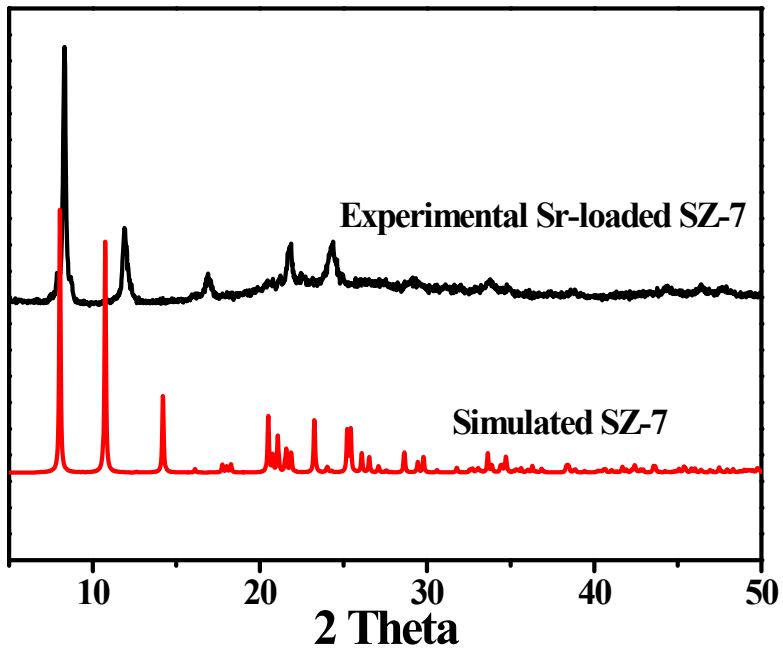

Figure S13. Powder X-ray diffraction patterns of experimental Sr-loaded SZ-7 samples.

Reference:

[1] N. E. Brese and M. O. Keeffe, *Acta Cryst.*, 1991, **B47**, 192-197.

[2] X. -H. Qi, K. Du, Z. M. Feng, J. -R. Li, C. F. Du, B. Zhang and X. Huang, *J. Mater. Chem. A*, 2015, **3**, 5665-5673.

[3] M. J. Manos, N. Ding and M. G. Kanatzidis, *Proc. Natl. Acad. Sci. U. S. A.*, 2008, **105**, 3696-3699.

[4] J. L. Mertz, Z. H. Fard, C. D. Malliakas, M. J. Manos and M. G. Kanatzidis, *Chem. Mater.*, 2013, **25**, 2116-2127.

[5] D. Sarma, C. D. Malliakas, K. S. Subrahmanyam, S. M. Islama and M. G. Kanatzidis, *Chem. Sci.*, 2016, **7**, 1121-1132.

[6] C. C. Pavel and K. Popa, *Chem. Eng. J.*, 2014, **245**, 288-294.

[7] J. Lehto and A. Clearfield, *Chem. Lett.*, 1987, **18**, 1-13.

[8] A. M. El-Kamash, *J. Hazard. Mater.*, 2008, **151**, 432-445.

[9] T. Wen, X. Wu, M. Liu, Z. Xing, X. Wang and A. W. Xu, *Dalton. Trans.*, 2014, **43**, 7464-7472

[10] J. Zhang, L. Chen, X. Dai, L. Zhu, C. Xiao, L. Xu, Z. Zhang, E. V. Alekseev, Y. Wang, C. Zhang, H. Zhang, Y. Wang, J. Diwu, Z. Chai and S. Wang, *Chem*, 2019, **5**, 977-994.

[11] Y.-J. Gao, M.-L. Feng, B. Zhang, Z.-F. Wu, Y. Song and X.-Y. Huang, *J. Mater. Chem. A*, 2018, **6**, 3967-3976.

[12] P. Asgari, S. H. Mousavi, H. Aghayan, H. Ghasemi and T. Yousefi, *Microchem. J.*, 2019, **150**, 104188.

[13] W. Mu, S. Du, X. Li, Q. Yu, R. Hu, H. Wei, Y. Yang and S. Peng, *Dalton. Trans.*, 2019, **48**, 3284-3290.

[14] N. Shen, Z. Yang, S. Liu, X. Dai, C. Xiao, K. Taylor-Pashow, D. Li, C. Yang, J. Li, Y. Zhang, M. Zhang, R. Zhou, Z. Chai and S. Wang, *Nat. Commun.*, 2020, **11**, 5571.